



## Heavy metal removal of intermittent acid mine drainage with an open limestone channel

A. Alcolea<sup>a,\*</sup>, M. Vázquez<sup>a</sup>, A. Caparrós<sup>a</sup>, I. Ibarra<sup>a</sup>, C. García<sup>b</sup>, R. Linares<sup>c</sup>, R. Rodríguez<sup>d</sup>

<sup>a</sup> Servicio de Apoyo a la Investigación Tecnológica, Universidad Politécnica de Cartagena, 30202 Cartagena, Murcia, Spain

<sup>b</sup> Departamento de Ingeniería Minera, Geológica y Cartográfica, Universidad Politécnica de Cartagena, 30203 Cartagena, Murcia, Spain

<sup>c</sup> Departamento de Geología, Universidad Autónoma de Barcelona, 08193 Bellaterra, Cerdanyola del Vallès, Barcelona, Spain

<sup>d</sup> Instituto Geológico y Minero de España, Ríos Rosas, 23, 28003 Madrid, Spain

### ARTICLE INFO

#### Article history:

Received 7 September 2011

Accepted 8 November 2011

Available online 3 December 2011

#### Keywords:

Acid rock drainage

Tailings

pH control

Environmental

Pollution

### ABSTRACT

This study is focused on the influence of a particular open limestone channel (OLC) on the quality of the surface water drained from an intermittent watercourse. The OLC was constructed along a creek surrounded by upstream tailings deposits, in an extensive, abandoned sulfide-mining site, which generates acidic and heavy metals-rich drainage water during the occasional precipitation that occurs. The overall length of the OLC is 1986 m, it has an average slope of 4.6%, and consists of two main segments. The effectiveness of this channel was evaluated through different physico-chemical parameters: pH, electrical conductivity (EC), total solids (TS), and heavy metal concentrations (Al, Fe, Zn, Ni, Cu, As, Cd, and Pb), measured in surface water. A total of 47 water samples were collected in 12 rainfall events, in the period 2005–2009. Moreover, for three different precipitation events, depletion curves of these parameters were constructed. The values of pH and Ca were increased downstream of the channel, related to the alkalinity and calcium release of the OLC and carbonates present in the watershed, whereas the EC, TS, K, Mg,  $\text{SO}_4^{2-}$ , Al, Mn, Fe, Ni, Cu, Zn, As, Cd, and Sb decreased towards the mouth of the creek. The OLC reduced the input of heavy metals into the Mar Menor lagoon by one order of magnitude. According to the results, this kind of constructive solution is effective with regard to mitigating the effects of intermittent acid mine drainage in Mediterranean and semi-arid regions.

© 2011 Elsevier Ltd. All rights reserved.

### 1. Introduction

Sierra de Cartagena-La Unión (Southeast Spain) contains one of the most important Pb–Zn accumulations in the Iberian Peninsula. This region has been mined from the Phoenician and Carthaginian times until 1991, using underground and open-pit mining techniques. The most frequent metallurgical process to recover valuable minerals from sulfide ores has been froth flotation, followed in importance by gravity separation. Mining activities have generated more than 200 Mm<sup>3</sup> of mine wastes, spread over an area of 9 km<sup>2</sup>. According to the type of mining activity, mineral processing and disposal methods, nine types of mining and metallurgical wastes can be distinguished: open-pit spoils, post-flotation wastes, gravity concentration spoils, “false” gossan dumps, molten slag, pre-concentration wastes, mine spoils, well borings, and post-flotation sludge (Robles-Arenas et al., 2006). Oxidation and hydrolysis of metal sulfides generate an intermittent acid mine drainage every rainfall event. In order to neutralize surface water acidity, reducing its pollution charge, a passive treatment system of almost 2 km has

been implemented over certain watercourse. This paper reports the effectiveness of this system from the point of view of the pollution reduction that enters the Mar Menor lagoon, a wetland included on the list of the Ramsar Convention (Duran et al., 2003) and in the Coastal Area Management Programme by the UN Environment Programme (Da Cruz and Murcia regional working group, 2003) for its ecological importance.

Acid mine drainage (AMD) water originates from the oxidation and weathering of sulfide deposits. These geological materials are, in most cases, multi-mineral aggregates, because they include a variety of minerals, such as aluminosilicates, oxides, hydroxides, phosphates, halides, and carbonates, apart from sulfides.

As far as generation of  $\text{H}^+$  is concerned, the weathering process of each single mineral can be classified as acid-producing (sulfide minerals, iron and aluminum hydroxides, and secondary sulfate minerals), acid-buffering (carbonates and certain aluminosilicates), or neutral (oxides, such as quartz, rutile, and zircon). The balance of all the chemical reactions occurring in a particular waste at a certain time will determine the final pH of the acidic, metal-rich pore water solution that drains into the watercourse (Lottermoser, 2007).

Rate of acid generation is determined by pH, temperature, oxygen concentration in gas and water phases, chemical activity

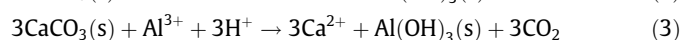
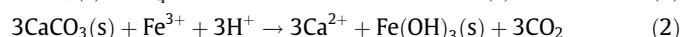
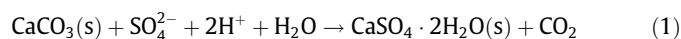
\* Corresponding author. Tel.: +34 968338955; fax: +34 968338952.

E-mail address: [alberto.alcolea@sait.upct.es](mailto:alberto.alcolea@sait.upct.es) (A. Alcolea).

of  $\text{Fe}^{3+}$ , surface area of exposed metal sulfide, chemical activation energy, and bacterial activity (Akil and Koldas, 2006). It is known that, above pH 3.5, oxidation of iron in mine drainage is not due to microbial activity (Hallberg, 2010). Therefore, a slight increasing of pH directly restricts one of the primary factors of acid generation.

Mining activities usually have a strong influence on natural waters. In particular, pollution of surface water due to leaching from tailings deposits demands close attention, due to the fact that some of its consequences can endure for many years after the abandonment of mining. Different types of mining impact on the water environment can be distinguished: mining *per se*, mineral processing and disposal of mine wastes, and post-mining flooding and uncontrolled discharge of polluted waters (Younger and Wolkersdorfer, 2004). In the particular creek and landscape that are the object of this study, the impact related to the disposal of mine wastes is the most significant. These products, with different particle sizes, ranging from coarse to fine-grained mineral processing wastes, are usually combined in extensive areas. The precipitation pattern – with occasional, heavy rainfall typical of a Mediterranean climate – leads to the physical and chemical instability of these tailings areas, producing intermittent, acidic, and metalliferous leachates, even when these zones have been revegetated.

Open limestone channels (OLCs) are passive treatment systems that achieve remediation mostly through chemical means (Kalin et al., 2006). They consist of a limestone bed rock and optimal performance is attained on slopes exceeding 12%, where the flow speed and turbulence keep precipitates in suspension (Skousen and Ziemkiewicz, 2005). Other passive systems are anoxic limestone drains, aerobic and anaerobic wetlands, and biological and abiotic permeable, reactive barriers (Johnson and Hallberg, 2005). Very often, an OLC is preferred due to its low building and maintenance costs. Carbonates from limestones and dolostones contribute to increasing the alkalinity and pH of AMD water, causing heavy metals to precipitate on them. Regrettably, this precipitation is accompanied with the formation of an armor of iron hydroxide, aluminum hydroxide, and gypsum that may decrease the permeability and reactivity of the calcareous rock (Ziemkiewicz et al., 1997; Hammarstrom et al., 2003). Furthermore, the rate of the neutralization reaction was observed to decrease dramatically with increasing pH, so that carbonate rocks are not very useful above pH of 5. Although attractive economically, a fresh reactive surface must continually be presented to the acidic mine drainage for neutralization to occur (Egiebor and Oni, 2007). Armoring processes can be represented by the following reactions:



Generally, OLCs are used to treat AMD under conditions of very-high flow, because continually-moving water may erode any armoring from the limestone (Pavlick et al., 2005). However, their usage with intermittent AMD water is very limited. This paper evaluates the effectiveness of this passive treatment, with regard to its use in other mining areas having semi-arid or Mediterranean climates.

## 2. Materials and methods

### 2.1. Location

The OLC that is the object of this study was built onto El Beal creek, an ephemeral watercourse located in the municipality of Cartagena (Region of Murcia, Southeast Spain), between the villages of Llano del Beal (to the east) and El Beal (to the west), and upstream of them. This creek is the main waterway that flows into the southern side of the Mar Menor lagoon, because it chan-

nels water coming from the El Llano and San Ginés mountains. These elevations belong to the Sierra de Cartagena-La Unión, a 2500-year-old mining district extended over an area of 100 km<sup>2</sup>. The wadi drains a wide watershed, which helps to carry a high volume of fine-grained materials (sand, silt, and clay) to the hypersaline lagoon. The El Beal creek is surrounded upstream by a wide variety of sulfide mine wastes, such as open-pit spoils, gravity concentration spoils, mine spoils, and post-flotation wastes (Fig. 1).

Table 1 shows some annual meteorological variables, averaged from 2000 to 2009, at Roche, the closest station to the creek. This station belongs to the SIAM network (SIAM, 2010, agrometeorological reports). Although these values are typical for a dry-summer, sub-tropical climate, 2009 was an extraordinarily 'rainy' year, with an overall precipitation of 543 mm.

When this study was initiated, three sampling points were chosen to monitor the effect of the channel on the surface waters: B1–B3. In December 2009, due to the unexpectedly-fast building of the second section of the channel, three new sampling locations were added, namely A–C (CARM, 2011, cartographic visor): see Fig. 2.

### 2.2. Timeline

The OLC was visited in the period December 2004 to December 2009, from the initial construction of the first section to the completion of the second section. From February 2005 through December 2009, the surface water running over it was monitored in the main rainwater events. Furthermore, in the period November 2006 to October 2007, two points were sampled repeatedly in the same event, in order to plot depletion curves of certain parameters. The flow patterns were often ephemeral, such that in the space of a few hours the flow ceased, regardless of the amount of precipitation that day. This explains why sometimes there was no surface water flowing at the time of sampling, even after a heavy rainfall. See the timeline of events below:

December 9, 2004: Building labors of the first section. It will measure 1184 m long.

February 9, 2005: Mouth of El Beal creek (B3). With 24 mm of rainfall that day there was surface water running.

February 10, 2005: In B3, after 2 days of rainfall (25 mm altogether), there was no surface water running.

November 15, 2005: After 6 days of rainfall (56 mm altogether), there was surface water running in B2, but not in B1 or B3.

January 7, 2006: After 2 days of rainfall (7 mm altogether), there was no surface water running in B1, B2, or B3.

January 28, 2006: After 2 days of rainfall (32 mm altogether), there was surface water running in B2 and B3, not in B1.

April 17, 2006: After 2 days of rainfall (23 mm altogether), there was surface water running in B1 and B2, not in B3.

May 4, 2006: After 3 days of rainfall (20 mm altogether), there was surface water running in B2, but not in B1 or B3.

September 14, 2006: After 3 days of intermittent precipitation (25 mm altogether), there was no surface water running in B1, B2, or B3.

November 3, 2006: Depletion study in El Beal creek. B1 was sampled four times and B2 five times. A total precipitation of 61 mm was recorded in 2 days. In B3, there was no surface water running.

March 27, 2007: Depletion study in El Beal creek. B1 and B2 were sampled five times. In B3, there was no surface water running. A total precipitation of 18 mm was recorded in 2 days of constant, weak rain.

October 18, 2007: Depletion study in El Beal creek. B1 and B2 were sampled five times, and B3 was sampled once. A total precipitation of 63 mm was recorded in 3 days of constant and weak rain.

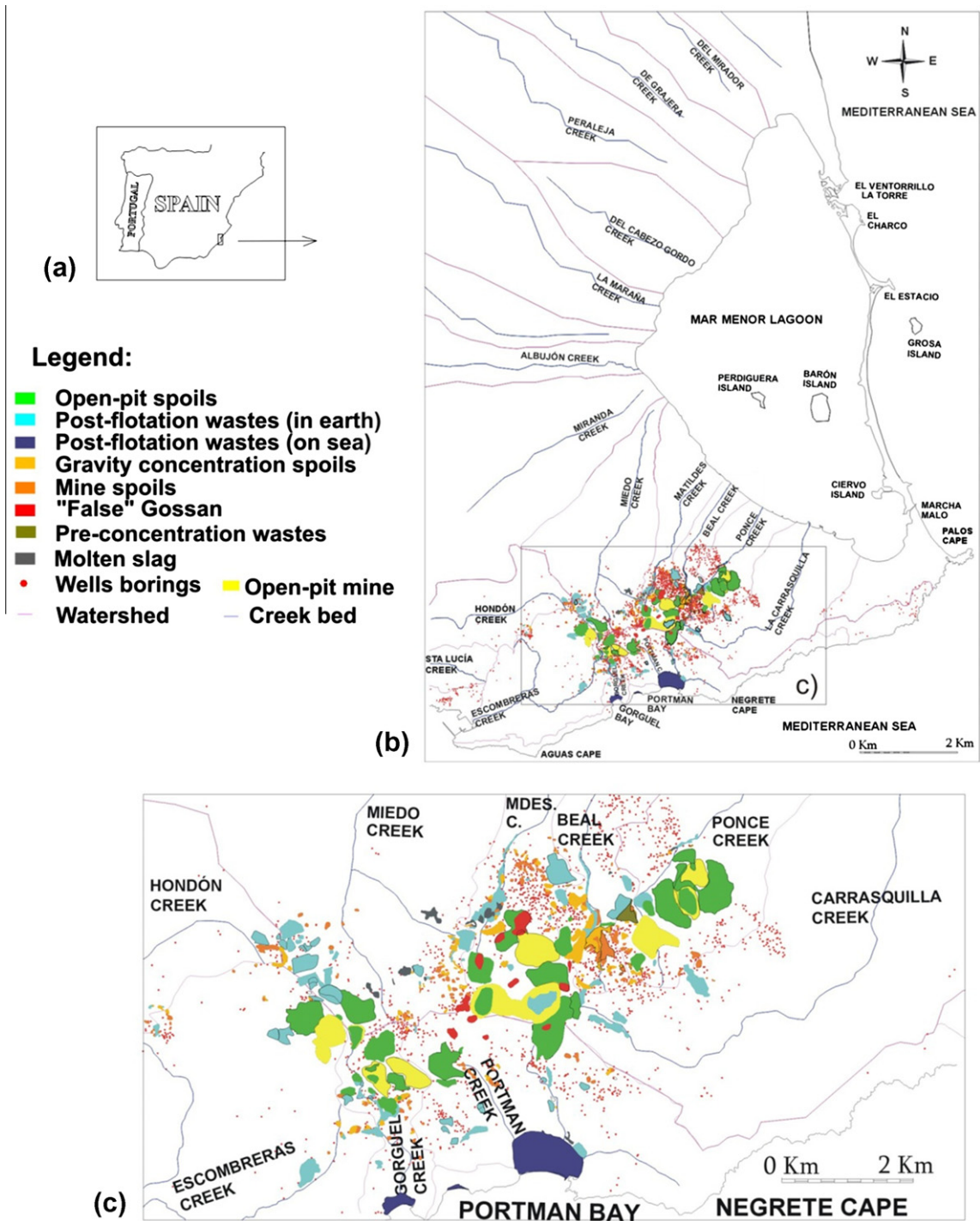


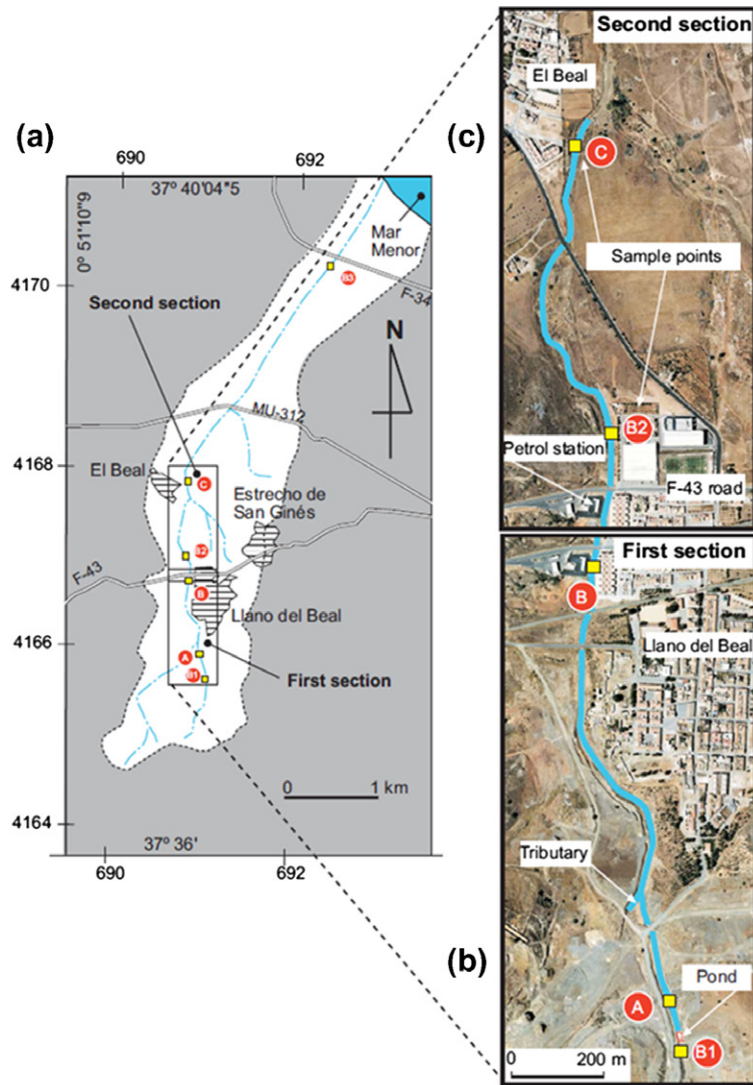
Fig. 1. (a) Study-area location, (b) area affected by mining activities and (c) distribution of mining and metallurgical wastes (García, 2004).

Table 1  
Annual meteorological variables,  $n = 10$ .

	$T (^{\circ}\text{C})$	Relative humidity (%)	Wind speed (m/s)	Wind direction ( $^{\circ}$ )	Precipitation (mm)	$ET_0$ (mm)
Average	17.5	70	1.9	116	380	1224
Standard deviation	0.4	2	0.2	26	115	51

$ET_0$  is the reference evapotranspiration, computed by the Penman–Monteith equation.





Datum: ETRS89. Projection: UTM-30. Z in meters above mean sea level.  
The source of the creek is located at (X, Y, Z) = (691147, 4164918, 240)

Code	X	Y	Z	Situation	Distance from the source (m)	Sampling period
B1	690942	4165542	150	Before the channel	671	Apr. 2006 - Nov. 2008
B2	690737	4166757	90	After the first section	1944	Nov. 2005 - Nov. 2008
B3	692342	4170142	4	Near the mouth	6107	Feb. 2005 - May 2008
A	690938	4165594	150	After the pond	713	December 2009
B	690740	4166604	98	At the end of the first section	1790	December 2009
C	690646	4167352	61	At the end of the second section	2622	December 2009

**Fig. 2.** (a) Map showing the six sampling points along the watershed of El Beal creek, (b) first section of the open limestone channel and (c) second section of the open limestone channel. Both sections are divided by the F-43 road.

May 8, 2008: After 2 days of rainfall (3 mm altogether), there was surface water running in B1 and B2, not in B3.  
May 31, 2008: After 2 days of rainfall (16 mm altogether), there was surface water running in B1–B3.  
November 30, 2008: After 2 days of rainfall (12 mm altogether), there was surface water running in B1 and B2, but not in B3.  
April 9, 2009: Visit to the first section of the channel. 4 years after the beginning of its construction, there are clear signs of silting in certain upper areas.  
December 12, 2009: Second section is completed. It is 802 m long and was built during 2009.

December 14, 2009: Surface water running in the channel was sampled in three positions: before its first section (A), at the end of the first section (B), and 100 m from the end of the second section (C). In 2 days there was a total precipitation of 89 mm.

### 2.3. Specifications and design

The overall length of the OLC is 1986 m, consisting of two sections. A 1184 m section ("first section") with a rectangular-like upstream pond, whose measurements are  $21 \times 10$  m (Fig. 3g), and

a short, left downstream tributary 45 m long (Fig. 3b). The second section, 802 m long, is located from Llano del Beal village to El Beal.

The purpose of the upper pond is to keep the gypsum, ferric and aluminum hydroxides in suspension, in order to avoid their deposition over the limestone (Ziemkiewicz et al., 1996; Green et al., 2008). In addition, there are several dams upstream of the OLC, and to enhance the reception of surface water before the pond there are two wings, each 3 m long, on each side of the upstream aperture. Furthermore, at the end of the channel there is a small dam and a 2 m height waterfall.

The large stones of the bed rock range from 60 to 150 cm in length. Stones on the walls range from 30 to 40 cm in length. The sides of the channel keep their shape because the stones are confined with wire netting, forming a gabion. The wire has a diameter of 3 mm and produces a net of irregular hexagons, with four sides of 6 cm and two sides of 3 cm each (Fig. 3f).

The section of the channel shows two lateral steps with different dimensions along the waterway (Fig. 4). The distance *e* becomes longer at the very end of the channel, where it is 12 m wide. The depth of the limestone bed rock is supposed to range between 0.5 and 1 m along the channel. Before the building of the channel, the creek was 1 m wide on average (Fig. 3c) and now is at least four times wider. Thus, the channeling labors involved widening of the creek bed, meaning that the surface water is in contact with the carbonate rocks for longer.

El Beal is the steepest creek of the five waterways flowing towards the Mar Menor lagoon from the Sierra de Cartagena-La Unión mining district. The creeks are named, from NW to SE, Miedo, Matildes, El Beal, Ponce, and Carrasquilla. The average slope in El Beal creek is 3.3%, while the first section of the channel has a slope of 4.6% and the second a slope of 4.5%.

## 2.4. Analytical techniques

### 2.4.1. Mineralogy of bed rocks

Fractured pieces of boulders collected from positions A–C (Fig. 2) were sampled from the central part of the channel, breaking the rocks with chisel and hammer, and extracting the final specimens avoiding the analysis of their armored surfaces. After sampling, the specimens were placed immediately in plastic bags, labeled, and sealed for transfer to the laboratory. The mineralogy was studied by X-ray diffraction (XRD) for phase identification, and by wavelength dispersive X-ray fluorescence spectrometry (WDXRF) for elemental analysis. Due to the measurement method and the optical configuration of the spectrometer, elements with atomic number less than 9 could not be measured directly. Instead, thermogravimetric analysis coupled to mass spectrometry (TG–MS) was carried out, mainly to distinguish the carbon dioxide and moisture in the samples – which helps to complete a good semi-quantitative analysis by WDXRF.

Specimens for XRD were air-dried and gently ground by hand with a mortar and pestle. Mineral phases were identified by powder XRD using a Bruker D8 Advance instrument in  $\theta$ – $\theta$  mode (Bruker Corporation, Billerica, MA, USA), with  $\text{CuK}\alpha$  radiation, 40 kV, 30 mA, and a scintillation detector. Samples were step-scanned from  $5^\circ$  to  $70^\circ$  in  $2\theta$ , with  $0.05^\circ$  stepping intervals, 6 s per step, and a rotation speed of 60 rpm. Powder samples were mounted in back-loading plastic holders. Diffraction patterns were evaluated with DIFFRAC<sup>plus</sup> software (specifically with EVA 12.0, a commercial package from Socabim, 2006) and powder diffraction files database PDF2 (ICDD, 2000).

Samples for WDXRF were dried at  $60^\circ\text{C}$  for 24 h (in order to release most of the free water) and then ground in a disc mill for 1 min, to give a final particle size of less than  $40\ \mu\text{m}$ . Sample preparation involved the formation of pressed-powder pellets using 5 g of sample and 0.4 g of binder (Margui et al., 2009). The

samples were analyzed using a commercial spectrometer (Bruker S4 Pioneer), equipped with a Rh anticathode X-ray tube (20–60 kV, 5–150 mA, and 4 kW maximum), five analyzer crystals ( $\text{LiF200}$ ,  $\text{LiF220}$ , Ge, PET, and XS-55), a sealed proportional counter for detection of light elements, and a scintillation counter for heavy elements. The energy resolution and efficiency for each analytical line were determined by both the collimator aperture and the analyzer crystal used. Analyses were performed in vacuum mode to avoid signal losses by air absorption, allowing the detection of low Z elements (González-Fernández et al., 2010). The recorded spectra were evaluated by the fundamental parameters method, using SPECTRA<sup>plus</sup> software linked to the equipment (specifically EVA 1.7, a commercial package from Bruker-AXS and Socabim, (Bruker AXS GmbH, 2006)). A standard-less method was used owing to the lack of satisfactory certified reference materials with metal concentrations in the same range as the rocks analyzed in this study. The use of standard-less procedures in the fundamental parameters method has been described by Rousseau (2001).

An advanced loss of ignition (LOI) study was performed using TG–MS. A “TGA/DSC 1 HT” thermogravimetric analyzer (Mettler-Toledo GmbH, Schwerzenbach, Switzerland) with a flowing oxygen atmosphere (50 ml/min) was used for this determination. The temperature was programmed to increase from  $30$  to  $1075^\circ\text{C}$  at  $30\ \text{K/min}$ , followed by an isothermal segment of 1 h at this temperature. All of the TGA measurements were blank-curve corrected and alumina pans of  $70\text{-}\mu\text{l}$  capacity, without lids, were used. The TGA instrument was coupled to a Balzers Thermostat mass spectrometer (Pfeiffer Vacuum, Asslar, Germany) for gas analysis. Only water vapor and carbon dioxide were analyzed. The dwell time for every ion was 10 s and the cathode voltage in the ion source was 65 V. A “QMS 200 M3” model quadrupole mass spectrometer was used (Alcolea et al., 2009).

### 2.4.2. Water analysis

A total of 47 surface water samples (250 ml each) were collected in El Beal creek in 12 rainfall events and at five different sampling positions, as shown in Section 2.2. For the collection, plastic bottles were filled completely (without an air space), tightly closed, and taken to the laboratory, where they were kept in a refrigerator until their analysis. The physico-chemical characterization involved determination of pH, electrical conductivity (EC), total solids (TS), and the metals of interest.

The samples for pH and EC determination were first filtered through a  $0.45\text{-}\mu\text{m}$  membrane, to remove particulate matter. The pH was measured with a Crison GLP 22 pH meter (Crison Instruments S.A., Barcelona, Spain) that was calibrated daily with standard solutions of pH 4.01 and 7.00, chosen because all the surface water samples evaluated were acidic. The EC was measured with a Crison GLP 32 conductimeter, which was calibrated daily with standards of  $1413\ \mu\text{S/cm}$  and  $12.88\ \text{mS/cm}$ , a range which covers most of the EC values of the surface water samples. Determination of TS was performed according to EPA method 160.3. (Keith, 1996).

Non-acidified samples were analyzed for major ions ( $\text{Na}^+$ ,  $\text{K}^+$ ,  $\text{Ca}^{2+}$ ,  $\text{Mg}^{2+}$ ,  $\text{Cl}^-$ ,  $\text{NO}_3^-$ , and  $\text{SO}_4^{2-}$ ) using the Metrohm 861 automated ion chromatography system (Metrohm, Herisau, Switzerland) equipped with conductometric detection and an autosampler (Metrohm 838 Advanced Sample Processor). Separation of anions was carried out with a Metrosep A Supp 5–250 column having a  $0.7\ \text{ml/min}$  flow of a carbonate/bicarbonate eluent ( $3.2\ \text{mM Na}_2\text{CO}_3 + 1.0\ \text{mM NaHCO}_3$ ). Cations were separated on a Metrosep C 2–250 column, with an eluent composition of  $4\ \text{mM}$  tartaric acid +  $0.75\ \text{mM}$  dipicolinic acid and a flow of  $1.0\ \text{ml/min}$ . The measured limits of detection (LOD) were  $2\text{--}60\ \mu\text{g/l}$  for anions and  $70\text{--}300\ \mu\text{g/l}$  for cations. Anions and cations were quantified through external calibration curves. Prior to measurement, the samples were





**Fig. 3.** (a) Building labors of the first section, by Llano del Beal village (December 9, 2004), (b) left tributary in the first section (February 8, 2005), (c) B2 before the construction of the second section (May 31, 2008), (d) mouth of El Beal creek with the Mar Menor lagoon at the bottom (February 10, 2005), (e) stratification in B2 (February 9, 2005), (f) limestone wall, held in place by wire netting, (g) pond at the beginning of the channel (January 7, 2006), (h) the previous pond with the bed rock silted-up (December 12, 2009), (i) a recently-broken part of a rock, 10 cm long, with an ochre profile due to contact with AMD water and (j) the landscaped way along the channel.

filtered through 0.2- $\mu\text{m}$  pore-diameter cellulose acetate membrane filters.

Metal concentrations were measured in samples that had been filtered through 0.45- $\mu\text{m}$ -pore filters. Solutions and dilutions were

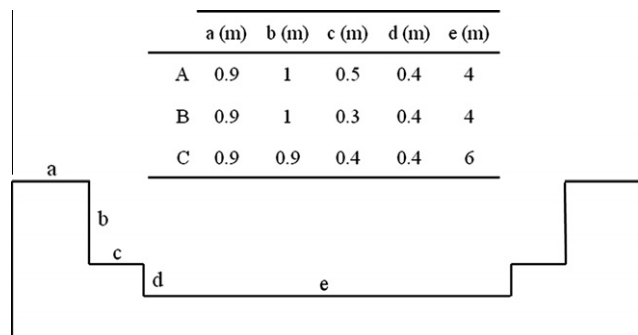


Fig. 4. Cross-section and dimensions (in m) of the channel at sampling points A–C.

prepared with purified water obtained from an Elix 3/Milli-Q Element system (Millipore, Billerica, MA, USA). All glassware and plastic materials used were treated previously for at least 24 h with 10% (v/v) high-purity nitric acid (Panreac, Barcelona, Spain) and then rinsed with purified water before use. The study was focused on eight metals (Al, Fe, Ni, Cu, Zn, As, Cd, and Pb), which were determined by inductively coupled plasma-mass spectrometry (ICP-MS). The analysis was performed using an Agilent 7500ce ICP-MS (Agilent Technologies, Santa Clara, CA, USA) equipped with an ASX-510 autosampler (Cetac Technologies Inc., Omaha, NE, USA). The samples were introduced into a Scott spray chamber using a MicroMist glass concentric nebulizer and then into a Fassel-type torch. An octopole reaction system (ORS), using He as collision gas, was employed to remove polyatomic interferences. The sample temperature was set at 2 °C and the radio frequency power was set to 1500 W. Argon (spectral purity, >99.998%) was used as the carrier gas, at a flow rate of 0.97 l/min. The sample was inserted and nebulized with a pump operated at 0.1 rotations per second (rps). The measurements were compared with standards to calculate metal concentrations. A multi-elemental solution with Sc, Ga, Tl, and Rh was used as internal standard to correct for drift over a series of runs. The concentrations of elements in the samples were determined in triplicate. An external-standard calibration method was applied to all determinations. Seven-point calibration curves were constructed by analyzing multi-element reference standards prepared from stock solutions (High-Purity Standards, Charleston, SC, USA). The precision and accuracy of this method were tested by analyzing the reference material CWW-TM-D, a Certified Waste Water Trace Metals Solution (High-Purity Standards). The relative error (RE%) of all analyzed elements was less than 6% for the values obtained in our laboratory. The good agreement with the certified values is shown in Table 2. The precision was determined by introducing the same quantity of one sample seven times. After that, the relative standard deviation was calculated (RSD%, between 0.69 and 2.42). Furthermore, every 10 samples, a standard was analyzed to check whether its concentration differed by more than 10% from its true value. If it did, the instrument was recalibrated. All these acceptance criteria agree with the EPA method (Method 6020A, US Environmental Protection Agency, 2007) and the manufacturer's procedures (Wilbur, 2007). The instrumental limits of detection were (μg/l) 0.79 for Al, 1.57 for Fe, 0.09 for Ni, 0.29 for Cu, 0.79 for Zn, 0.07 for As, 0.03 for Cd, and 0.25 for Pb.

### 3. Results

#### 3.1. Mineralogy of bed rocks

Three samples of limestone from the bed rock were analyzed for the mineralogical study in positions A–C (Fig. 2). Ochre deposition on the surface of the boulders was more evident upstream.

Carbonate rocks at positions A and B are pale gray in color and dark gray at position C. The XRD patterns show that the dominant mineral is calcite at positions A and B, with small amounts of quartz and muscovite, while at C dolomite is the only crystalline phase (Fig. 5).

The WDXRF ( $Z > 8$ ) and TG–MS ( $\text{CO}_2$  and  $\text{H}_2\text{O}$ ) analyses show CaO, MgO, and  $\text{CO}_2$  values typical of calcite at positions A and B, while the values for C are in good agreement with those of ideal dolomites (Table 3).

#### 3.2. Water analysis

A statistical summary of surface water data along the El Beal creek is shown in Table 4. This includes samples collected from February 2005 to November 2008, when only the first section of the channel was completed. Compared to World Health Organization guidelines for drinking-water quality (WHO, 2008), the samples were characterized by low pH (2.4–4.2),  $\text{Na}^+$  (1–13 mg/l),  $\text{K}^+$  (63–188 mg/l),  $\text{Cl}^-$  (27–43 mg/l),  $\text{NO}_3^-$  (4–7 mg/l), and Sb values (2–5 μg/l), and by high EC (2691–14,010 μS/cm), TS (6–40 g/l),  $\text{Ca}^{2+}$  (379–488 mg/l),  $\text{Mg}^{2+}$  (126–564 mg/l),  $\text{SO}_4^{2-}$  (2665–24,515 mg/l), Al (77–2047 mg/l), Mn (49–212 mg/l), Fe (0.3–1252 mg/l), Ni (89–2821 μg/l), Cu (170–13,351 μg/l), Zn (291–3290 mg/l), As (1–854 μg/l), Cd (379–5356 μg/l), and Pb concentrations (252–1125 μg/l).

The overall trend was for water quality to improve with increased treatment distance. For example, the values of pH and Ca increased towards the mouth, related to the alkalinity and Ca release by the OLC and the carbonates present in the watershed. Also, the values of EC, TS, K, Mg,  $\text{SO}_4^{2-}$ , Al, Mn, Fe, Ni, Cu, Zn, As, Cd, and Sb decreased downstream. This downward trend is particularly noticeable with Fe and As, whose values were reduced by three orders of magnitude. In spite of this tendency to decline, the  $\text{SO}_4^{2-}$ , Al, Mn, Zn, Cd, and Pb concentrations in the mouth of the creek were still one or two orders of magnitude higher than guideline values.

The exception to this general decrease for heavy metals was Pb, since its concentration increased four-fold along the first OLC segment and then slowly decreased towards the mouth of the creek. It can be assumed that this rise in concentration is not related to the contribution of the AMD, because Pb is associated mineralogically with other chemical elements that should show the same rising tendency.

Basin, depletion, and timeline curves were plotted to evaluate the influence of the limestone channel on the quality of the surface water that flows over it. The parameters considered were pH, EC, TS, and metal concentrations.

Only the metals Al, Fe, Zn, Ni, Cu, As, Cd, and Pb were selected for the preparation of the different curves (Mn and Sb were excluded for the lack of data). The sums of metals were grouped into minor-fraction analytes (Al, Fe, and Zn) and micro-fraction analytes (Ni, Cu, As, Cd, and Pb). The minor-fraction metals ( $M_m$ ) can reach maximum concentrations ranging from 0.1% to 10%, that is,  $10^3$ – $10^5$  mg/l, and the micro-fraction metals ( $M_\mu$ ) can reach values of 1– $10^3$  mg/l (Müller et al., 2001).

##### 3.2.1. Basin curves

These five-point curves plot the average values of the analytical parameters versus the distance from the source of the creek. They take into account the effect of the second OLC segment, at points 1.8 and 2.6 km. Fig. 6 shows the positive influence of the OLC (located between 0.7 and 2.6 km) on all the parameters except for Pb concentration, because there is apparently an additional source of this metal.

Points 2 and 4 (sampling positions B and C) seem to follow a slightly different pattern than points 1 and 3 (sampling positions B1 and B2), because they belong to different sampling periods

**Table 2**

The accuracy and precision of the ICP-MS analyses of the certified reference material CWW-TM-D and the detection limits (DL) for the analytes.

Element	Isotope <sup>a</sup>	Measured values ( <i>n</i> = 7)					%RSD <sup>b</sup>	Certified Value	DL	%RE <sup>c</sup>
		Min	Max	Median	Mean	S.D.				
Al	27	197.72	204.06	198.66	199.71	2.33	1.17	200	0.786	−0.14
Fe	56	195.75	206.08	203.32	202.74	3.60	1.77	200	1.573	1.37
Ni	60	198.50	202.45	201.40	201.00	1.38	0.69	200	0.086	0.50
Cu	63	194.84	200.41	198.97	198.31	2.25	1.13	200	0.291	−0.85
Zn	66	198.42	203.62	202.44	201.51	2.03	1.01	200	0.788	0.76
As	75	48.50	51.80	50.56	50.28	1.21	2.42	50	0.066	0.57
Cd	111	48.98	50.62	49.59	49.69	0.56	1.13	50	0.026	−0.62
Pb	208	202.12	216.70	211.64	210.47	4.63	2.20	200	0.249	5.23

Concentrations are in µg/l.

<sup>a</sup> Isotopic mass of element measured during analysis.

<sup>b</sup> Relative standard deviation.

<sup>c</sup> Relative error.

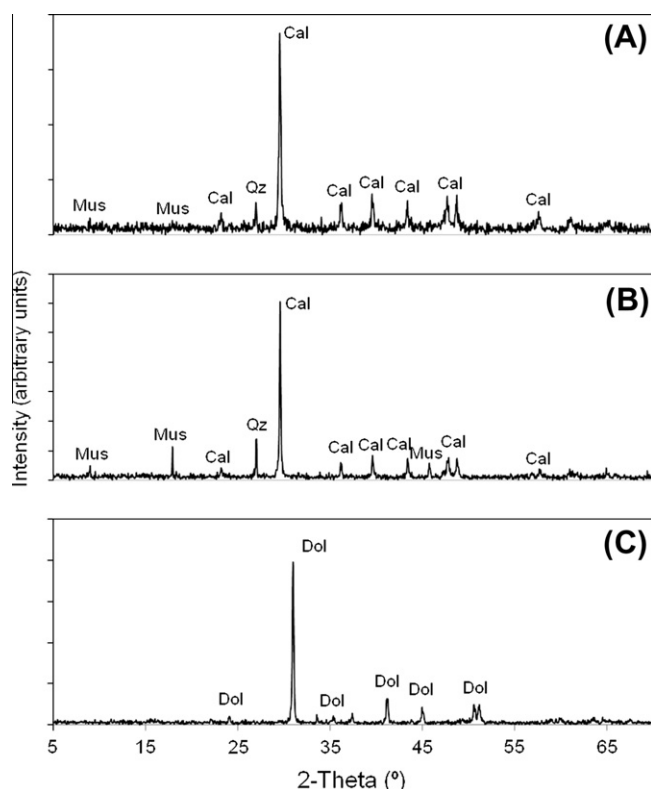


**Fig. 5.** X-ray powder diffraction patterns for carbonate rocks from positions A–C. The intensity is in arbitrary units for comparison. (Mus: Muscovite; Cal: Calcite; Qz: Quartz; Dol: Dolomite).

(Fig. 2). In spite of that, it is worth comparing them because five-point curves give far more information than three-point curves.

In Fig. 6d and e, the decreases in the absolute metal concentrations can be observed. Considering the minor-fraction metals, the effectiveness of the OLC declines in the order Zn > Al > Fe. Nevertheless, using the after OLC-before OLC ratios, the order of efficiency is Fe > Al > Zn. Regarding the micro-fraction metals, the order of effectiveness for the absolute values is Cu > Cd > Ni > As, while for the after OLC-before OLC ratios, the order is As > Cu > Ni > Cd. For Pb, the limestone channel was ineffective, its curve showing a maximum at the end of the second section of the OLC.

### 3.2.2. Depletion curves

These five-point curves describe how the declining flow rate in the creek affected the performance of the OLC. Three important rainfall events were chosen, with an average precipitation of 47 mm, from November 2006 to October 2007, a period in which

**Table 3**

Bulk composition of carbonate rocks at positions A, B, and C, determined by WLXRF and TG-MS (wt.%).

Oxides	Z	A	B	C	Calcite	Dolomite
H <sub>2</sub> O	1	0.62	0.19	0.06		
CO <sub>2</sub>	6	40.40	39.25	46.77	43.97	47.73
Na <sub>2</sub> O	11	0.05	0.08	<0.01		
MgO	12	0.94	0.86	19.12		21.86
Al <sub>2</sub> O <sub>3</sub>	13	1.69	2.41	0.36		
SiO <sub>2</sub>	14	2.60	3.46	0.86		
SO <sub>3</sub>	16	0.13	0.20	0.06		
Cl	17	0.01	0.01	0.04		
K <sub>2</sub> O	19	0.51	0.62	0.09		
CaO	20	52.02	51.54	31.22	56.03	30.41
TiO <sub>2</sub>	22	0.06	0.06	0.01		
MnO	25	0.01	0.01	0.30		
Fe <sub>2</sub> O <sub>3</sub>	26	0.55	0.61	1.08		
SrO	38	0.37	0.64	<0.01		
Total		99.97	99.94	99.96		

only the first section of the channel had been finished. Points B1 and B2 were sampled alternately ten times (five cycles) during 2.5 h, every rainfall event. Every parameter is averaged for the three rainwater episodes.

Fig. 7a shows that the flow and its depletion are greater downstream (B2 values are higher than B1 ones and slope is more negative for B2 than for B1). This phenomenon provokes a longer retention time of the surface water on the OLC. Thus, pH was increased (Fig. 7b) at B2 and, consequently, all the metal concentrations decreased with the drop in flow (Fig. 7e–k and m–n). The exception, again, was Pb, because it is the only metal with a positive slope at B2 (Fig. 7l). The Fe concentration was insensitive to flow changes at B1, but at B2 it decreased exponentially with the reduction in the rate of water flow (Fig. 7f).

The separation of the lines in every graph represents the effectiveness of the OLC for the parameter studied. As a result, for instance in the TS graph (Fig. 7d), the two lines are closer together because they are unrelated to the effectiveness of the channel and the gap depends only on the slight difference in the local topographic slopes at B1 and B2. On the other hand, there is a relatively wider separation of the lines for the minor-fraction (Fig. 7m) than for the micro-fraction metals (Fig. 7n). Both metal fractions exhibit the general tendency that the slopes of the B2 lines are almost insensitive to the drop in flow, with the exceptions of Fe and Pb (for different reasons and with different signs).

### 3.2.3. Timeline curves

The period of study was February 2005 to December 2009, although the data for metals start in November 2005. The vertical lines in Fig. 8 are related to the depletion study. This series of



**Table 4**  
Statistics of surface waters chemical data along E1 Beal creek before the building of the second section of the OLC.

	B1					B2					B3					G.D.W.
	N	Av	Min	Max	SD	N	Av	Min	Max	SD	N	Av	Min	Max	SD	
pH	18	2.4	2.1	2.7	0.2	21	3.6	2.6	4.3	0.4	3	4.2	3.5	6.1	0.7	(6.5–9.5)
EC ( $\mu\text{S}/\text{cm}$ )	18	14,010	6840	22,700	6389	21	4410	2620	10,860	1971	3	2691	930	4030	1188	(2500)
Q (l/s)	18	0.27	0.00	2.00	0.54	21	1.98	0.10	4.00	1.24	3	2.07	0.20	4.00	1.90	
TS (g/l)	18	39.55	11.31	98.28	27.21	22	14.26	5.75	77.68	15.23	4	6.06	3.29	13.11	5.62	(1.2)
Na <sup>+</sup> (mg/l)	6	1.46	0.07	6.01	2.43	6	13.01	7.47	24.49	6.48	3	9.10	6.71	10.50	2.09	(200)
K <sup>+</sup> (mg/l)	6	188.42	0.30	280.98	102.36	6	113.10	0.30	213.65	78.64	3	62.94	32.04	101.28	35.22	(150)
Ca <sup>2+</sup> (mg/l)	6	379.43	252.85	470.77	98.71	6	488.43	428.53	536.38	41.16	3	433.22	319.18	492.10	98.72	(200)
Mg <sup>2+</sup> (mg/l)	6	564.32	403.72	696.34	126.07	6	295.79	171.86	528.69	146.71	3	125.53	63.57	189.66	63.08	(50)
Cl <sup>-</sup> (mg/l)	6	26.92	11.03	41.20	11.08	6	43.24	24.26	65.75	14.56	3	26.98	25.66	27.64	1.14	(250)
NO <sub>3</sub> <sup>-</sup> (mg/l)	6	4.08	0.01	20.70	8.22	6	6.62	1.44	21.10	7.24	3	4.30	2.29	5.66	1.78	50
SO <sub>4</sub> <sup>2-</sup> (mg/l)	6	24514.96	13209.49	36878.00	9418.14	6	6339.66	3820.99	11288.49	3068.11	3	2665.16	1487.09	4100.39	1325.49	(250)
Al (mg/l)	18	2046.81	436.40	4884.00	1443.67	21	205.88	25.59	703.60	162.81	3	76.93	19.21	189.10	97.16	(0.1)
Mn (mg/l)	3	212.23	119.80	290.90	86.38	3	103.49	54.26	170.20	59.91	3	49.01	17.44	84.25	33.56	0.4
Fe (mg/l)	18	1251.76	511.20	2816.00	821.83	21	9.06	0.10	67.19	15.42	3	0.33	0.08	0.52	0.23	(3)
Ni ( $\mu\text{g}/\text{l}$ )	19	2820.90	99.70	7526.00	1357.13	22	451.78	102.80	2116.00	444.03	3	88.64	45.60	144.50	50.67	70
Cu ( $\mu\text{g}/\text{l}$ )	19	13351.00	406.00	42680.00	6769.50	22	1246.88	97.80	3977.00	1120.23	3	170.48	16.90	448.50	241.21	2000
Zn (mg/l)	19	3290.00	777.39	6611.00	1606.53	22	727.85	291.00	2126.00	496.63	3	290.81	80.44	502.90	211.24	(3)
As ( $\mu\text{g}/\text{l}$ )	19	854.10	20.60	5355.90	541.78	22	3.73	0.05	20.10	5.22	3	1.12	0.10	2.20	1.07	10
Cd ( $\mu\text{g}/\text{l}$ )	19	5355.74	322.30	28330.20	4180.68	22	1684.61	314.40	8572.00	1706.56	3	378.52	97.40	698.10	302.21	3
Sb ( $\mu\text{g}/\text{l}$ )	4	5.09	2.48	11.55	5.21	3	2.20	1.96	2.67	0.41	3	2.21	1.88	2.55	0.34	20
Pb ( $\mu\text{g}/\text{l}$ )	19	251.59	9.20	10219.90	2306.30	22	1124.85	9.90	2365.90	601.28	3	613.37	237.40	1087.00	433.14	10

N valid sample size, AV average, Min minimum, Max maximum, SD standard deviation, G.D.W. WHO guideline for drinking water quality – values in parentheses are not based on health considerations, but on unacceptable limits for taste, aesthetics or corrosion of facilities-.

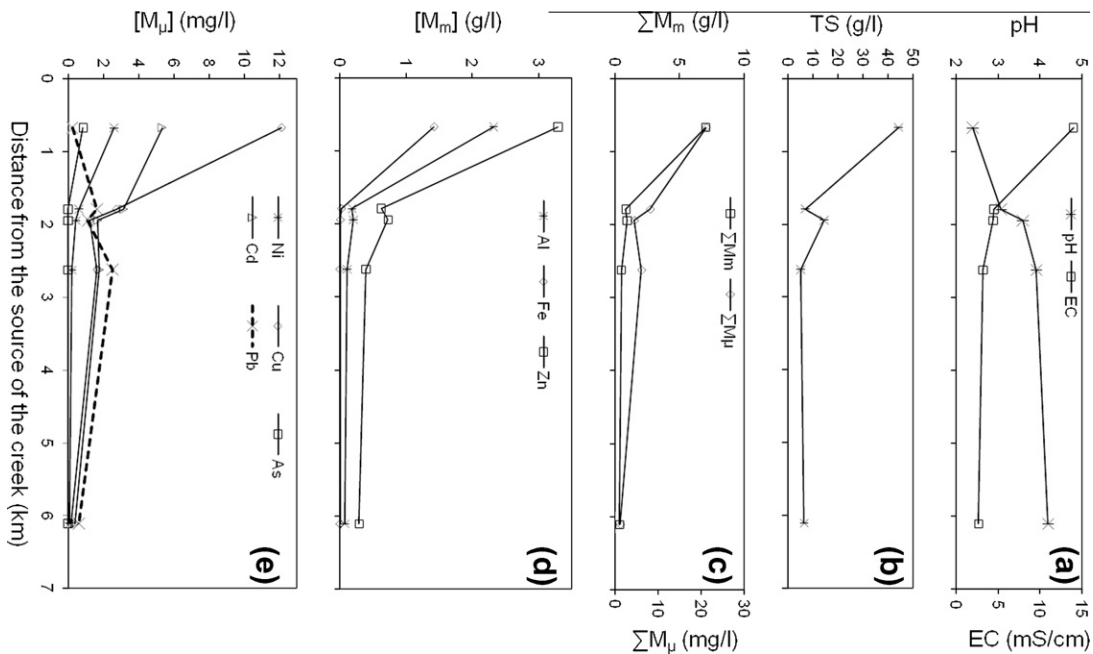


**Fig. 6.** Evolution of several averaged parameters along E1 Beal creek. The OLC is between 0.7 and 2.6 km from the source of the creek. (a) pH and electrical conductivity, (b) total solids, (c) sums of minor- and micro-fraction metals, (d) Al, Fe, and Zn concentrations and (e) Ni, Cu, Cd, and Pb concentrations.

curves shows the effect of the entire OLC, even though only the final month includes the effect of the second segment.

In Fig. 8a, the increment in precipitation along the period of study can be appreciated, with the characteristic pattern of a sub-tropical climate: relatively-wet falls and dry summers. In these 4 years, the pH at B2 and B3 exhibited a tendency to decrease, probably due to the accumulation of sediments on the bed rock, linked to the low average slope of the channel and the absence of maintenance. As a result of this, the metal concentrations remained stable or increased at B2 and increased slightly at B3, without exception (Fig. 8d–m). The TS decreased with time, because the increase in rainfall diluted the solids transported by the surface water (Fig. 8c).

The values of all the variables decreased with time at B1, except for pH – which remained constant despite the dilution effect related to the rise in rainfall and the extent of the weathering of the mine residues upstream.

#### 4. Discussion

All the curves shown in Figs. 6–8 illustrate the positive influence of the limestone channel on the AMD water. Nevertheless,

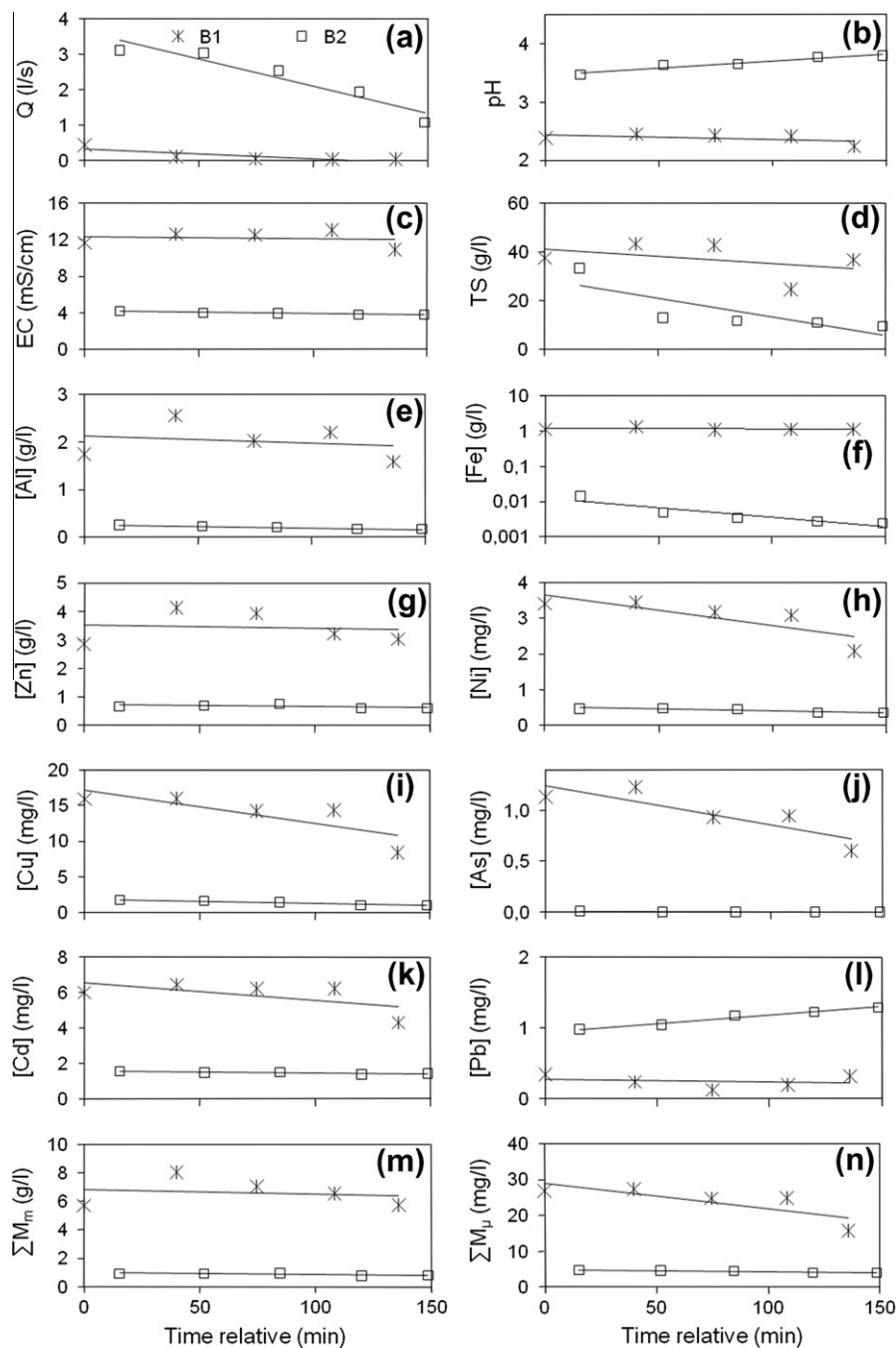


**Fig. 7.** Depletion curves before (B1) and after (B2) the first segment of the OLC on El Beal creek. (a) flow, (b) pH, (c) electrical conductivity, (d) total solids, (e) Al concentration, (f) Fe, (g) Zn, (h) Ni, (i) Cu, (j) As, (k) Cd, (l) Pb, (m) sum of minor-fraction metals and (n) sum of micro-fraction metals.

this influence was unable to reduce the high values of  $\text{SO}_4^{2-}$ , Al, Mn, Zn, Cd, and Pb found in the mouth of the creek. Regarding the depletion phenomenon, the effectiveness of the channel was not sensitive to the fast draining of surface water; an improvement in performance was seen only for Fe. Furthermore, the OLC exhibited stable behavior over these 5 years, despite the accumulation of sediments upstream.

Ziemkiewicz et al. (1997) showed that steeper channels neutralized more acidity because the iron coating was thinner or was continuously scoured out from the surface of the bed rock. On the other hand, longer channels with a greater residence time seem to be more effective at reducing acidity (McDonald et al., 2001). Rose and Lourenso (2000) showed that OLCs as short as 127 m and with a slope of only 4.4% could be effective.

Four years after its construction began, the OLC on El Beal creek is still effective, even though its first segment is silted-up with sediments. The reason for this effectiveness has to do with its length, which, together with a gentle slope (4.6%, far from the desirable > 12%), makes a long residence time possible. Besides, rainfall events are usually so intensive and short that the inlet flow rate is reduced by 2/3 in only 2 h, which increases residence time and, therefore, effectiveness.

No efflorescences were found on the bed rock surface in the dry seasons. These secondary sulfate minerals constitute an acidity reservoir which could neutralize the effectiveness of the carbonates and decrease pH again (Bernier et al., 2001). Nevertheless, the light coloration, up to 5-cm deep, at the boulder surfaces had become ochre (Fig. 3i) due to the precipitation of iron hydroxides.

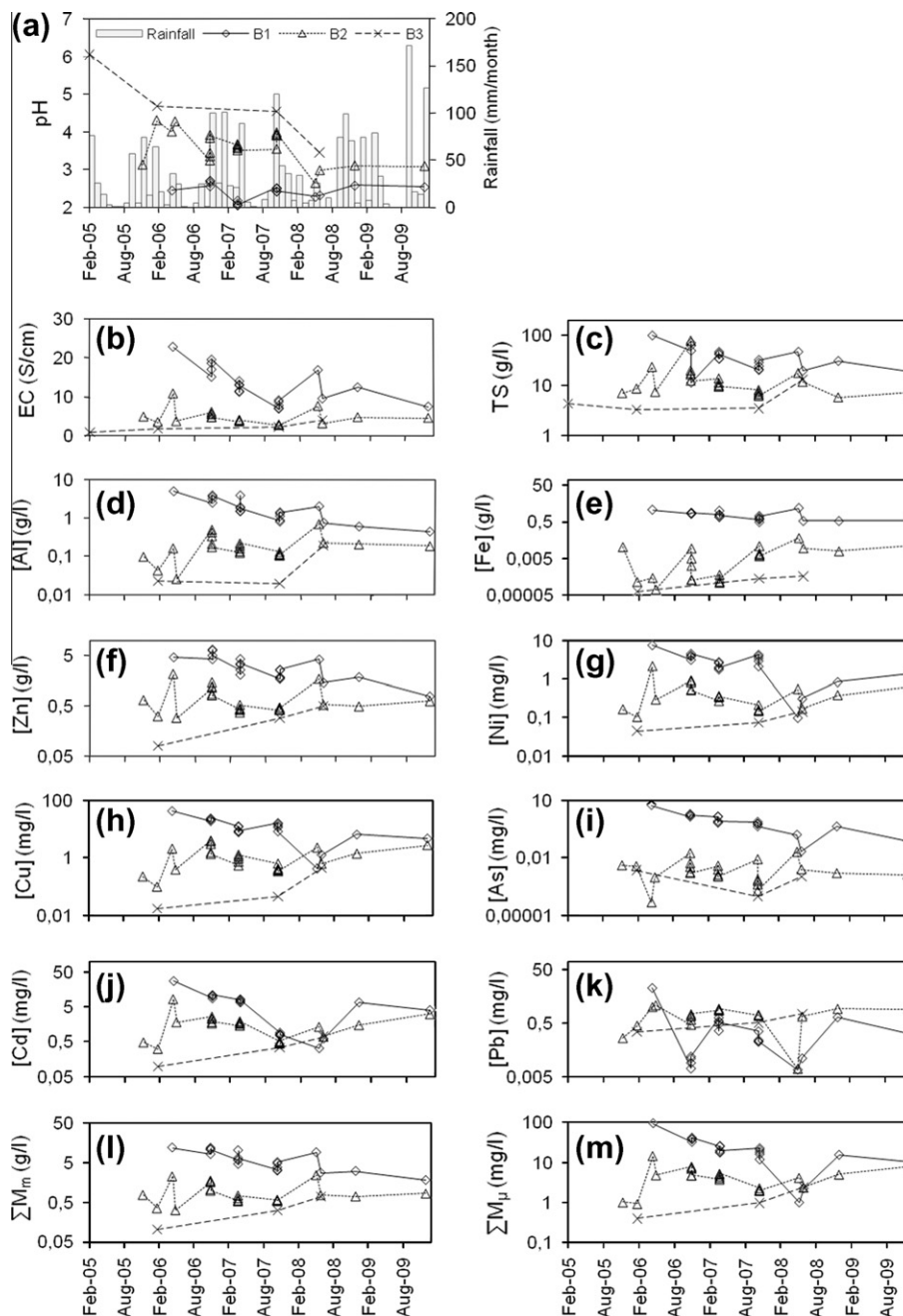


**Fig. 8.** Timeline curves before the OLC (B1), after the first segment (B2), and near the mouth (B3) in El Beal creek. (a) Variation of pH and monthly rainfall, (b) electrical conductivity, (c) total solids, (d) Al concentration, (e) Fe, (f) Zn, (g) Ni, (h) Cu, (i) As, (j) Cd, (k) Pb, (l) sum of minor-fraction metals and (m) sum of micro-fraction metals.

This mechanism favors the removal of harmful metals (Ni, Cu, Zn, and Pb) by adsorption or co-precipitation, at a pH at which they would normally remain in solution (Coulton et al., 2003).

The mineralogical analysis confirmed that the first section of the OLC consists of limestones and that the second is composed mainly of dolostones. Both these carbonate rocks are abundant throughout the area, because the Sierra de Cartagena-La Unión belongs to the Internal Zones of the Betic Cordillera, a region whose different geological complexes are rich in carbonated members (García-Tortosa et al., 2000; Kager, 1980). Hence, due to its proximity, building the channel with this kind of material is an inexpensive solution for alleviating the effect of intermittent AMD in these ephemeral watercourses.

Fig. 3g and h shows that nearly 1 year was enough for the silted material to prevent the contact of AMD water with the bed rock in the upper pond. This is the reason why a maintenance protocol for the removal of this layer of silt should be performed on a yearly basis, to keep the surface of the limestone active. A method to remove periodically the sediment from the bed rock could improve the effectiveness of the system. A sediment trap could be set up across the channel to collect the residues and prevent them from being transported downstream. Another option is a permeable geotextile cover over the limestone, which could be shaken occasionally and raised up to eliminate the sediment. Taking into account the frequency and intensity of the rainfall events, performance of this task once or twice a year would be enough.



## 5. Conclusions

The Sierra de Cartagena-La Unión is a landscape greatly affected by mining labors. Mining and the metallurgical industry need an effective treatment of the residues that generate AMD, both during the mining activities and after their conclusion. Very often, these sites have no closure plan when operating and may induce a considerable environmental impact. Abandoned residues give rise to an intensive pressure on the environment. As a consequence of weathering processes, there is a strong deterioration of surface and subterranean waters.

An OLC was built to mitigate the effect of intermittent AMD on the El Beal creek and Mar Menor lagoon. The prevailing rainfall pattern, with intensive but short rainfall events, enables the effectiveness of the channel, even though, 5 years since the construction of the first segment, approximately 50% of the surface of this section appears silted-up, mainly in the upper areas. The creek bed is not steep enough to prevent the accumulation of sediments on top of the limestone, but the gentle slope of the OLC is compensated by the long length of the channel, which produces a longer residence time of the surface water on the calcareous rocks. The surfaces of the bed boulders have undergone a slight change in color, from the original white to the current ochre, but there are no secondary sulfate mineral efflorescences on them. The analytical results illustrate that the armoring process on the carbonate rocks has not inactivated their alkalinity. However, in the face of the sediment accumulation, maintenance activities, to remove material and avoid future accumulation on the bed rocks, are necessary.

Most of the results shown in this paper have to do with the effectiveness of the first segment of the OLC. Currently, the length of the channel is almost double what it was and its effectiveness should be greater. An OLC is a low-cost solution to the effects of intermittent AMD on the quality of surface water in Mediterranean and semi-arid mining areas, although it does not offer a complete solution. The concentrations of analytes like  $\text{SO}_4^{2-}$ , Al, Mn, Zn, Cd, and Pb exceed in one or two orders of magnitude the World Health Organization guidelines for drinking-water quality in the mouth of the creek. For Pb, the OLC is particularly inefficient, due to the possible presence of an additional source of this metal in the area, unrelated to the AMD.

Finally, it is worth emphasizing the positive esthetic effect of channeling on the surrounding villages, because the building of the OLC in this ephemeral watercourse has involved other benefits, such as landscape gardening and the design of green spaces for recreation purposes.

## Acknowledgements

The authors gratefully acknowledge the infrastructural support of the Assistance Service for Technological Research of the Universidad Politécnica de Cartagena (Spain). We also thank Dr. David-James Walker from Institute for Research and Agrarian Development of Murcia (IMIDA-Murcia) for the thorough language revision of this manuscript.

## References

Akcil, A., Koldas, S., 2006. Acid Mine Drainage (AMD): causes, treatment and case studies. *Journal of Cleaner Production* 14, 1139–1145.

Alcolea, A., Ibarra, I., Caparrós, A., Rodríguez, R., 2009. Study of the MS response by TG–MS in an acid mine drainage efflorescence. *Journal of Thermal Analysis and Calorimetry* 101, 1161–1165.

Bernier, L., Aubertin, M., Dagenais, A.M., Bussiere, B., Bienvenu, L., Cyr, J., 2001. Limestone drain design criteria in AMD passive treatment: theory, practice and hydrogeochemistry monitoring at Lorraine Mine Site, Temiscamingue. In: IM Minespace annual meeting proceedings technical paper 48. CIM, Quebec, p. 9.

Bruker AXS GmbH. DIFFRAC<sup>plus</sup> EVA 2006. Bruker AXS GmbH, Karlsruhe, Germany.

CARM. Comunidad Autónoma de la Región de Murcia. Infraestructura de datos espaciales de referencia de la Región de Murcia (IDERM). <http://www.cartomur.com/visorcartoteca> (verified 8 Aug. 2011).

Coulton, R.H., Bullen, C., Hallet, C.J., 2003. The design and optimization of active minewater treatment plants. *Land Contamination and Reclamation* 11, 273–279.

Da Cruz, H., Murcia regional working group, 2003. Programme for the integrated management of the Mar Menor coastline and its area of influence. Feasibility study. UNEP, Region of Murcia and Mediterranean action plan, 136 pp. [http://www.pap-thecoastcentre.org/camp-definitivo\\_ing.pdf](http://www.pap-thecoastcentre.org/camp-definitivo_ing.pdf) (verified 8 Aug. 2011).

Duran, J.J., García de Domingo, A., López-Geta, J.A., 2003. Hydrogeological characterization of the Spanish wetlands included in the Ramsar Convention. 1:2,500,000 Map. Geological Survey of Spain.

Egiebor, N.O., Oni, B., 2007. Acid rock drainage formation and treatment: a review. *Asia Pacific J. Chem. Eng.* 2, 47–62.

García, C., 2004. Impacto y riesgo ambiental de los residuos minero-metalúrgicos de la Sierra de Cartagena-La Unión (Murcia-España). Ph.D. thesis, Universidad Politécnica de Cartagena, Spain.

García-Tortosa, F.J., López Garrido, A.C., Sanz de Galdeano, C., 2000. Las unidades alpujarrides y maláguides entre Cabo Cope y Cabo de Palos (Murcia, España). *Geogaceta* 28, 67–70.

Green, R., Waite, T.D., Melville, M.D., Macdonald, B.C.T., 2008. Effectiveness of an open limestone channel in treating acid sulfate soil drainage. *Water Air and Soil Pollution* 191 (1–4), 293–304.

González-Fernández, O., Jurado-Roldán, A.M., Queralt, I., 2010. Geochemical and mineralogical features of overbank and stream sediments of the Beal wadi (Cartagena-La Unión mining district, SE Spain): Relation to former lead–zinc mining activities and its environmental risk. *Water Air and Soil Pollution* 215 (1–4), 55–65.

Hallberg, K.B., 2010. New perspectives in acid mine drainage microbiology. *Hydrometallurgy* 104, 448–453.

Hammarstrom, J.M., Sibrell, P.L., Belkin, H.E., 2003. Characterization of limestone reacted with acid-mine drainage in a pulsed limestone bed treatment system at the Friendship Hill National Historical Site, Pennsylvania, USA. *Appl. Geochem.* 18, 1705–1721.

ICDD. Powder Diffraction File Release 2000 Data Sets 1–50 plus 70–88. International Center for Diffraction Data, Newtown Square, PA, USA.

Johnson, D.B., Hallberg, K.B., 2005. Acid mine drainage remediation options a review. *Science of the Total Environment* 338 (1–2), 3–14.

Kager, P.C.A., 1980. Mineralogical investigation on sulfides, Fe–Mn–Zn–Mg–Ca–carbonates, greenalite and associated minerals in the Pb–Zn deposits in the Sierra de Cartagena, Province of Murcia. SE Spain. Ph.D. thesis, University of Amsterdam, GUA paper of Geology series 1(12):230.

Kalin, M., Fyson, A., Wheeler, W.N., 2006. The chemistry of conventional and alternative treatment systems for the neutralization of acid mine drainage. *Science of the Total Environment* 366, 395–408.

Keith, L.H., 1996. Compilation of EPA's Sampling and Analysis Methods second ed. CRC/Lewis: Boca Raton.

Lottermoser, B.G., 2007. Mine wastes: characterization, treatment and environmental impacts (second ed.). Springer, Heidelberg. pp. 33–51.

Margui, E., Queralt, I., Van Grieken, R., 2009. X-ray fluorescence analysis, sample preparation for. In: R. A. Meyers (Ed.) *Encyclopedia of analytical chemistry: Applications, theory, and instrumentation*. New York, Wiley Interscience. pp. 20.

McDonald, L., Sun, Q., Skousen, J., Ziemkiewicz, P., 2001. Water quality prediction model in open limestone systems. In: Xie, Wang, Jiang (Eds.) *Computer applications in the mineral industries*. Lisse: Swets & Zeitlinger. pp. 279–282.

Methods for determination of inorganic analytes: Inductively Coupled Plasma–Mass Spectrometry (Method 6020A), 2007. EPA Test Methods on-line (SW-846). <http://www.epa.gov/epawaste/hazard/testmethods/sw846/pdfs/6020a.pdf> (verified 8 Aug. 2011).

Müller, H., Zwanziger, H.W., Flachowsky, J., 2001. Trace analysis. In: Günzler H., Williams A., editors. *Handbook of analytical techniques*. Weinheim, Germany: Wiley-VCH Verlag GmbH. p. 110.

Robles-Arenas, V.M., Rodríguez, R., García, C., Manteca, J.I., Candela, L., 2006. Sulphide-mining in the physical environment: Sierra de Cartagena-La Unión (SE Spain) case study. *Environmental Geology* 51, 47–64.

Rose, A.W., Lourenso, F.J., 2000. Evaluation of two open limestone channels for treating acid mine drainage. In: Paper presented at the 2000 National Meeting of the American Society for Surface Mining and Reclamation, Florida.

Rousseau, R.M., 2001. Detection limit and estimate of uncertainty of analytical XRF results. *Rigaku Journal* 18 (2), 33–47.

Pavlick, M., Hansen, E., Christ, M., 2005. Watershed based plan for the North Fork Blackwater River watershed, West Virginia. Downstream strategies; Morgantown, WV.

SIAM. Sistema de Información Agraria de Murcia. <http://siam.imida.es> (verified 8 Aug. 2011).

Skousen, J., Ziemkiewicz, P., 2005. Performance of 116 passive treatment systems for acid mine drainage. In: Proceedings of National Meeting of the American Society of Mining and Reclamation, Breckinridge. pp. 1100–1133.

WHO, 2008. Guidelines for drinking-water quality, third ed., vol. 1. Recommendations; Geneva, Switzerland: World Health Organisation.

Wilbur, 2007. Rapid analysis of high-matrix environmental samples using the Agilent 7500cx ICP–MS. Agilent Technologies, Inc.; Bellevue, WA, USA.

- Younger, P.L., Wolkersdorfer, C., 2004. Mining impacts on the fresh water environment: Technical and Managerial Guidelines for Catchment Scale Management. *Mine Water and the Environment*, vol. 23. Springer-Verlag. pp. S2–S80.
- Ziemkiewicz, P.F., Brant, D.L., Skousen, J.G., 1996. Acid mine drainage treatment with open limestone channels. Paper presented at the 13th Annual Meeting of the American Society for Surface Mining and Reclamation, Successes and Failures: Applying Research Results to Insure Reclamation Success, Tennessee.
- Ziemkiewicz, P.F., Skousen, J.G., Brant, D.L., Sterner, P.L., Lovett, R.J., 1997. Acid mine drainage treatment with armored limestone in open limestone channels. *Journal of Environmental Quality* 26, 1017–1024.